energies

*Article*

# Origin of Calcite Cements in Tight Sandstone Reservoirs of Chang 8 Member of the Yanchang Formation in Zhijing-Ansai Area, Ordos Basin, China

**Zehan Zhang [1], Kelai Xi [1,*], Honggang Xin [2], Chunming Yang [3], Hui Zhao [1], Youcheng Wang [1], Weidong Dan [2] and Bin Luo [2]**

[1] Key Laboratory of Deep Oil and Gas, China University of Petroleum, Qingdao 266580, China
[2] Research Institute of Petroleum Exploration & Development, PetroChina Changqing Oilfield Company, Xi'an 710065, China
[3] Xi'an Changqing Chemical Group Co., Ltd., Xi'an 710018, China
* Correspondence: xikelai@upc.edu.cn

**Abstract:** Calcite cement is a common type of cementation in tight sandstone reservoirs of the Upper Triassic Yanchang Formation Chang 8 Member in the Zhijing-Ansai area of the Ordos Basin, which has significant influence on reservoir densification and heterogeneity. Calcite cements affect the quality of the reservoir conspicuously. The characteristics and origins of calcite were investigated using a series of approaches from the perspective of petrography and geochemistry, including thin section observation and identification, cathode luminescence, scanning electron microscopy, AMICS analysis, LA-ICP-MS elements analysis, and carbon and oxygen isotopes analysis. The results of all analytical tests indicated that calcite cements can be divided into two types according to their occurrence and origins. Type-I calcite cements mainly occur in sandstone reservoirs near the sandstone–mudstone interface or the sandstone layers adjacent to mudstone. Generally, there is no chlorite coating around them, and they appear dark orange under cathode luminescence. The carbon source of Type-I calcite cements may be related to the compaction and drainage of mudstone. Type-II calcite cements are formed in the early stage, and their carbon source may be related to the compaction and drainage of the adjacent mudstone. Type-II calcite cements are surrounded by chlorite coating primarily present in the interior of fine-grained sandstone, showing as bright yellow under cathode luminescence. Decarboxylation of organic matter in the source rocks may provide a crucial source of carbon for Type-II calcite cements.

**Keywords:** calcite cements; reservoir heterogeneity; tight sandstone reservoir; Yanchang Formation; Ordos Basin



**Citation:** Zhang, Z.; Xi, K.; Xin, H.; Yang, C.; Zhao, H.; Wang, Y.; Dan, W.; Luo, B. Origin of Calcite Cements in Tight Sandstone Reservoirs of Chang 8 Member of the Yanchang Formation in Zhijing-Ansai Area, Ordos Basin, China. *Energies* **2022**, *15*, 9544. https://doi.org/10.3390/en15249544

Academic Editor: Rouhi Farajzadeh

Received: 28 October 2022
Accepted: 14 December 2022
Published: 15 December 2022



## 1. Introduction

The Ordos Basin is one of the most important energy and mineral bases in China. It is rich in oil, coal and natural gas resources. Its reservoirs are characterized by wide distribution, multiple oil-bearing formations, low porosity and low permeability. The Yanchang Formation of the Upper Triassic in the Mesozoic Triassic is the main oil-bearing formation in the basin and is the key horizon in oil and gas exploration and development research. The Zhijing-Ansai area is located in the south central part of the Ordos Basin, mainly including Wuqi County, Zhidan County and Ansai District. Tight sandstone reservoirs with low porosity and permeability are mainly what has developed in the study area [1–5].

In recent years, significant progress has been made in the exploration of the Chang 8 oil-bearing formation in the Zhijing-Ansai area. Since 2020, the newly increased predicted reserves have exceeded 300 million tons, the large-scale oil-bearing enrichment area has been implemented and new replacement resources have been excavated for the stable

production of the old area. It has also become a significant area for the Ansai Oilfield to achieve the goal of increasing reserves and production in the next step, with good exploration prospects.

Carbonate cementation plays a vital role in affecting the quality and heterogeneity of tight sandstone reservoirs and also has an important impact on the reservoir space. Carbonate cementation has typical characteristics of wide distribution, multiple phases and complex geneses. Common carbonate cements include calcite, ferroan calcite, dolomite, ankerite, siderite, etc. [6,7]. A sedimentary environment and diagenetic fluids control and affect the difference of distribution of carbonate cementation jointly. Different microscopic characteristics and geochemical elements can reflect different sedimentary environment conditions and fluid properties for the formation of carbonate cements [8]. Sources of carbonate cements are various, sedimentary water, pore fluids outside sandstone reservoirs and alteration products of sandstone clastic particles, all these can be regarded as the sources for carbonate cements during diagenetic evolution [7–10].

Previous studies have concluded that the influence of carbonate cements on the properties of tight sandstone reservoirs has a dual character. On the one hand, when the content of carbonate cements in the early stage is within a certain range, compaction can be inhibited and the compression resistance of the reservoir is enhanced, which contributes to the preservation of the primary pores, and also provides a material basis for dissolution afterwards. In this way, the contents of secondary dissolution pores are increased and the physical properties of the reservoir are improved [6–10]. On the other hand, when the content of carbonate cement goes beyond a certain range, cements occupy a large amount of pore space in the reservoir, thus reducing the connectivity among pores, and greatly destructing the physical properties of the sandstone reservoir, leading to the densification of the reservoir eventually [9,10]. In the summary, despite the beneficial impact of carbonate cement in supporting the facies framework against mechanical compaction and hence increasing the intergranular volume, pervasive precipitation of calcite cements block, the intergranular pore spaces. Especially the calcite cements, they typically act to commonly enhance the reservoir quality and the pore connectivity by resisting and reducing compaction to some extent and smoothing pore walls [11–13]. Carbonate cements are usually concentrated in the middle and lower part of the fining-upward sandstone or near the interface from sandstone to mudstone or the layers that are rich in carbonate bioclasts. Distribution of carbonate cements also has impacts on the reservoir quality [14–16].

According to the exploration and development achievements in recent years, the Chang 8 sandstone reservoirs of the Yanchang formation are typical tight sandstone reservoirs with low porosity and permeability, but some reservoirs with high porosity also exist [8]. Sandstone reservoirs of the Chang 8 Member of the Yanchang formation in Zhijing-Ansai area are tight sandstone. Due to the stable distribution and wide extension of sandstone bodies, the Chang 8 sandstone is relatively thick, and at the same time, the reservoir is adjacent to the high-quality hydrocarbon source rocks of the Chang 7 Member. So, the reservoir reserves are considerable, and it is one of the most important objects of tight oil and gas exploration and development in the Ordos Basin, with good exploration prospects. Carbonate cements generally exist in the Chang 8 reservoir, and its content, distribution characteristics and formation stages directly affect the properties and hydrocarbon accumulation patterns of the reservoir [17–19].

At present, the origin and mechanism of carbonate cementation in tight sandstone reservoirs of the Chang 8 Member in Zhijing-Ansai area have not been sufficiently investigated, few studies focus on the Zhijing-Ansai area in the study of the Triassic Yanchang Formation in the Ordos Basin. Therefore, the innovation of this study is to focus on the tight sandstone reservoir of the Chang 8 Member of the Yanchang Formation in the Zhijing-Ansai area and conduct detailed characterization, material source and genetic mechanism research on calcite cements in the reservoir from macro- and microperspectives. The objectives of this study are to (1) investigate the petrologic and distribution characteristics of carbonate cementation and (2) clarify the origins of carbonate cementation.

The possible disadvantage or limitation is that this study is highly targeted and lacks generality; the object is a single type of cementation in tight sandstone reservoirs. Therefore, the research results may not universally applicable to conventional reservoirs. From a good point of view, this study can supplement and further improve the theories about the genetic mechanism of calcite cementation, lay a foundation for clarifying the diagenetic evolution sequence of tight sandstone reservoirs and help to determine the impact of calcite cementation on the reservoir.

This study may deepen our understanding of the characteristics and genesis of calcite in tight sandstone reservoirs in the Zhijing-Ansai area and has guiding significance for the prediction of high-quality reservoirs and the exploration and development of oil and gas resources in the study area and provides strong support for the determination of reservoir densification and prediction of high-quality reservoirs.

## 2. Geological Background

The Ordos Basin starts from Yinshan Mountain in the north, adjacent to Qinling Mountain in the south, borders Liupanshan Mountain in the west, and reaches Luliang Mountain in the east (Figure 1A). It is located in the west of the North China platform. It is a Mesozoic sedimentary basin formed on the pre-Mesozoic North China epicontinental sea craton basin. The Ordos Basin is one of the typical inland depression sedimentary basins and the second largest sedimentary basin in China. The Zhijing-Ansai area is located in the south central part of the Ordos Basin. Due to the large overall scope, the whole study area is further divided into three small blocks, namely, the Wuqi, Zhidan and Ansai areas from west to east, according to geographical location for the convenience of the study. From the perspective of tectonic location, the Zhijing-Ansai area is located in the first level tectonic unit of the Ordos Basin–Shanbei slope, which has a stable structure, relatively gentle terrain and is nearly north–south extended. The slope has a gentle monoclinal structure with a dip angle of less than 1° [20,21], and a low amplitude nose uplift structure can be seen locally (Figure 1A). A river–deltaic–lacustrine depositional system was developed in the Ordos Basin in the late Triassic, and the strata of the Yanchang Formation experienced the evolution process of formation, development and extinction of lacustrine basin during the sedimentary period. The upper Triassic Yanchang Formation is the main oil-bearing formation, which also can be divided into 10 oil-bearing formations (Chang 1–Chang 10) from top to bottom. The Chang 8 oil-bearing formation can be divided into two small layers, Chang $8_1$ layer and Chang $8_2$ layer, with a total sedimentary thickness of 70–105 m. The upper part lithologies of the Chang 8 reservoir are mainly dark grey mudstone and siltstone mixed with grey fine-grained sandstone. The lower part lithologies of the Chang 8 reservoir are mainly grayish yellow fine-grained sandstone mixed with gray silty mudstone and siltstone. Generally, the lithological association of the Chang 8 reservoir showing gray sandstone, dark mudstone and thin coal seam interbeddings developed (Figure 1B), belonging to typical shallow deltaic sedimentary facies [22–24].

The Chang 8 oil-bearing formation is adjacent to the source rocks of the Chang 7 Member, which formed during the settlement period of the stable development of the lacustrine basin. Sufficient supply of the provenance, the stable tectonic setting and the gentle terrain created beneficial conditions for the development of the Chang 8 reservoir system, forming a large-scale continuous lithologic oil-gas reservoir, which has good exploration prospects [23].

However, the Chang 8 reservoir has also experienced a relatively complex diagenetic evolution process, especially the destructive impact of carbonate cementation on the reservoir performance. As a result, the Chang 8 reservoir is now generally characterized by tight lithologies, poor physical properties, diverse pore types, a complex structure and strong heterogeneity, which restricts the efficiency of oil and gas production and its quality [24]. This paper mainly focuses on the south of the basin, including the Wuqi, Zhidan and Ansai areas (Figure 1A).

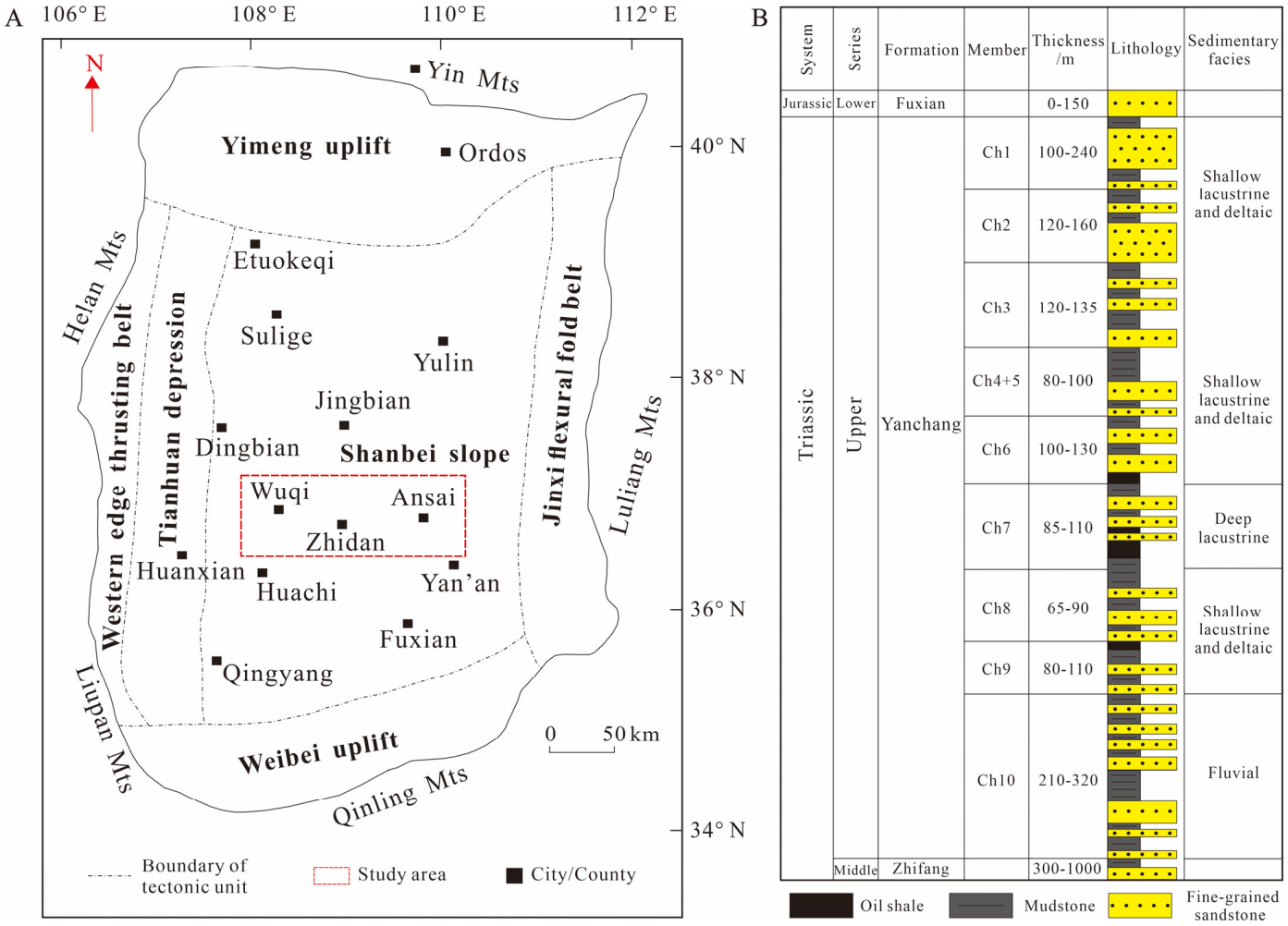


**Figure 1.** Location map and generalized Upper Triassic Yanchang Formation stratigraphy of the Ordos Basin. (**A**) Location of the Ordos Basin. (**B**) Generalized Upper Triassic Yanchang Formation stratigraphy of the Ordos Basin. Ch—Chang, Mts—Mountains.

## 3. Databases and Methods

All the data used in this paper were collected from the Research Institute of Petroleum Exploration and Development, Changqing Oilfield Company, PetroChina and tested in the Key Laboratory of Deep Oil and Gas, China University of Petroleum (East China) or other professional laboratories. The methods of sample selection are as follows. Firstly, based on the geographical distribution range of the study area, the principle of combining geographical location with sedimentary characteristics was adopted to select and determine typical wells, so as to ensure that Wuqi, Zhidan and Ansai area all had wells located in different sedimentary facies belts from south to north and from east to west. This principle also ensures the universality and applicability of the research results in the study area. Secondly, during the process of core sampling, we mainly noted the lithology and sedimentary structure of the core samples, as well as the different depths range of each well as reference. Generally, two or three rock samples were chosen from each meter of rock core. That is to say, one rock sample was taken every 30–45 cm within the depth range with roughly the same lithology and no obvious change in sedimentary structure. In case of a sudden lithological change, the interface of facies sequence change, or the typical sedimentary symbols, and so forth, the number of core samples were increased at the positions where typical changes occurred according to the actual situation. About 200 conventional core samples of 32 wells were collected from the Wuqi, Zhidan and Ansai areas. About 136 samples from sandstone and mudstone were made into blue

epoxy resin-impregnated thin sections for observation under the microscope using Zeiss polarized electron microscope, some were semistained with alizarin red dye solution for the identification of carbonate cements.

### 3.1. Cathode Luminescence (CL)

Cathode luminescence technology is mainly used to observe the different color characteristics of different types of calcite cements. Therefore, the sandstone samples with high calcite content were selected for experiments. Through microscopic thin section identification, most of the samples in the study area contained calcite to varying degrees. Therefore, in the 136 thin sections, the samples without calcite and with very little calcite were excluded; we carried out observations and tests under cathode luminescence on the remaining 89 samples. The machine type was a Camera bridge CL8200 MK5 detector. The parameter settings included the acceleration voltage of 10 KV, the beam current of 250 mA, the exposure time of 30–60 s, and the magnification of 50×, 100×, and 200×, respectively. The polished thin sections were observed and identified to further determine the type of calcite cements and their corresponding cathode fluorescence characteristics.

### 3.2. Scanning Electron Microscopy (SEM) and Energy Dispersive Spectrometer (EDS)

Scanning electron microscope observation and energy dispersive spectrum analysis were carried out to better identify the micromorphology, the element characteristics of calcite cements and the surrounding clay coatings, respectively. Therefore, 33 typical sandstone samples of two types of calcite were selected for testing and analysis according to the petrological characteristics of the thin sections. These 33 thin sections can clearly show whether there are chlorite coatings around calcite cements, and this contributes to the identification of mineral types and its geochemistry information. Before being used for testing, the surface of the thin sections was coated with metallic coatings. The metallic coatings were platinum coatings with nanometer thickness, and the single coating time was about 10 s. The purpose of the metallic coatings was to enhance the surface conductivity of the samples, so that the images would be clearer under the electron microscope. The Coxem EM-30 scanning electron microscope was used to observe and analyze the diagenetic minerals and pore space characteristics. The machine type of energy dispersive spectrometer was Crossbeam 550. The acceleration voltage was 20 keV, and the magnification was 100×–10,000×. In combination with the energy spectrometer (EDS), the morphological characteristics of quartz, calcite, chlorite and other minerals were clarified. The characteristics of chemical elements can be semiquantitatively characterized under the electron microscope, and the shape, size and distribution of pores can be recognized and characterized.

### 3.3. Mineral Scanning Analysis

AMICS scanning analysis and SEM-element surface scanning analysis can obtain accurate distribution and content characteristics of diagenetic minerals. In total, 10 typical sandstone samples which had obvious diagenetic phenomena were selected. The samples were chosen for composition analysis using a machine called Bruker AMICS-Mining system and for elements distribution analysis using a machine named Bruker Q200-XF6-100. The thin sections were all coated with platinum coatings to improve the conductivity of the sample surface. Combined with BSE images and energy dispersion spectrum (EDS) characteristics of the same field of view, the mineral types and content characteristics were identified precisely, as well as their corresponding chemical elements composition.

### 3.4. LA-ICP-MS Geochemical Elements Analysis

The main purpose of the test is to determine the geochemical characteristics of two different types of calcite cements. So, sandstone samples rich in calcite cements in different facies sequence positions were selected for major and trace element analysis. The thin sections were coated with metallic coatings in advance. The metallic coatings were nanoscale

platinum coatings. The purpose of the metallic coatings was to enhance the surface conductivity of the samples for the accuracy of the test. According to the observation results of the thin sections, 38 typical sandstone samples were selected for the major and trace elements analysis of carbonate minerals. The content of calcite cements in these 38 samples was of medium–high degree. The machine types were the laser denudation system of GeolasPro 193 nm and Agilent 7900 mass spectrometer. Laser ablation inductively coupled plasma mass spectrometry (LA-ICP-MS) was used to detect the contents of major, trace elements and rare earth elements of carbonate minerals. The thickness of selected representative thin sections was about 0.1 mm. The laser sampling analysis was carried out using a GeoLas2005 system with a cylindrical volume of about 40 $cm^3$. The operating conditions of the laser included a repetition frequency of 8 Hz and an energy density of 10 $J/cm^2$. The beam spot size of each analysis point was 44 μm. The background acquisition time was about 20 s (gas blank), and the subsequent data acquisition time was about 50 s. There were 40 kinds of major, trace and rare earth elements determined in total. The sandstone samples from different wells, different depths and different sedimentary facies sequences were analyzed to clarify the geochemical characteristics, which can be used to explain the source or genetic mechanism of carbonate cementation.

### *3.5. Carbon and Oxygen Isotopes*

Carbon and oxygen isotopes testing is performed to determine the carbon source of calcite cements, considering that the selected samples can cover the whole study area and the calcite content is not too low, combined with the petrographic characteristics, 46 typical sandstone samples containing carbonate cements were finally chosen for carbon and oxygen isotopes analysis and testing. The main equipment used was the isotope mass spectrometer host MAT-253. The sample preparation system was Kiel IV carbonate device. The experimental conditions were laboratory controlled room temperature in a range of 21–23 °C. Humidity was about 50% and RH ± 5%. The selected samples were sandstone samples that did not contain organic matter and carbonate debris, and came from different wells, different depths, different sequence positions and lithology. The allowable deviation of carbon isotope result was $\leq \pm 0.2$‰ and was $\leq \pm 0.3$‰ for the oxygen isotope. The carbon and oxygen stable isotopes data were represented by δ, corresponding to the Vienna Peedee belemnite (VPDB) standard.

## 4. Results

### *4.1. Reservoir Petrography*

The tight sandstone of the Chang 8 reservoir mainly includes mudstone, argillaceous siltstone, silty mudstone, siltstone, fine sandstone and medium-fine sandstone, which are dominated by siltstone and fine sandstone. Fine sandstone is the most commonly developed lithology of the reservoir. The mineral composition of the Chang 8 sandstones mainly consist of quartz, feldspar, rock fragments, cements and other minerals. The sorting of the tight sandstone is moderately well to well sorted. The roundness of detrital grains is subangular to subrounded.

The core samples in the study area are mainly dark gray black and gray white (Figure 2B,C). Based on core observation, thin section identification (Figure 2D,E) and the spots counting methods, the results show that the quartz proportion ranges from 28.47% to 33.53%, with an average of 31.86%. The feldspar grains proportion ranges from 40.02% to 50.97%, with an average of 45.08%. The rock fragments proportion accounts for 12.8% to 19.26%, with an average of 15.27%. The rock type is dominated by lithic feldsarkose (Figure 2A).

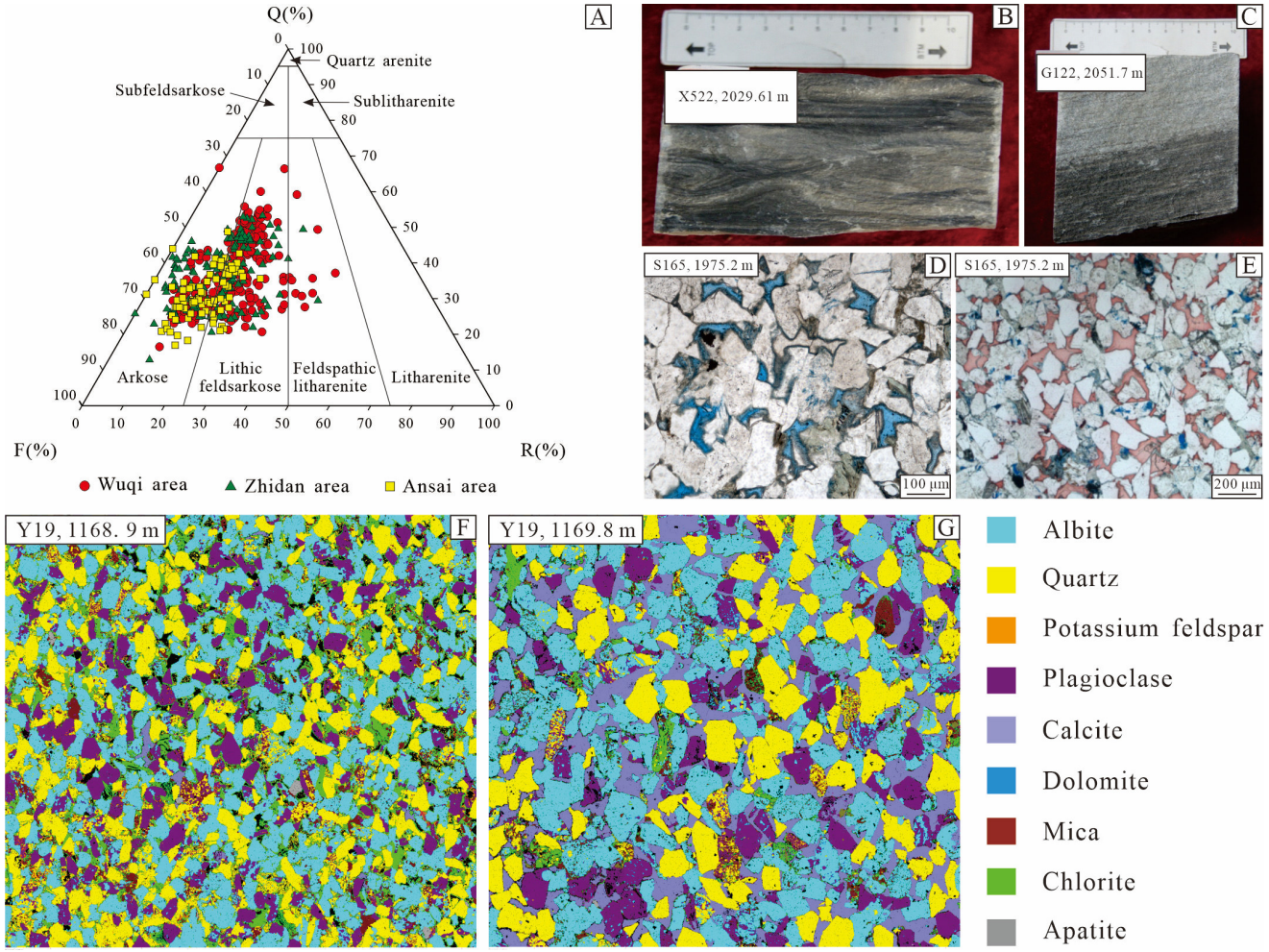


**Figure 2.** Rock compositions of Chang 8 Member of the Yanchang Formation tight sandstone reservoirs. (**A**) The ternary plot suggesting the rock types of tight sandstone reservoirs in the Yanchang Formation (Folk, 1980). (**B**) Photograph of rock samples from X522. (**C**) Photograph of rock samples from G122. (**D**) Photomicrograph of thin sections under plane-polarized light suggesting petrologic features of the sandstones, blue areas represent primary pores. (**E**) Photomicrograph of thin sections under plane-polarized light suggesting petrologic features of the sandstones, pink areas represent calcite cements. (**F**) Quantitative analysis of minerals using scanning electron microscope photomicrographs suggesting the mineral compositions from sample Y19 (1168.9 m). (**G**) Quantitative analysis of minerals using scanning electron microscope photomicrographs suggesting the mineral compositions from sample Y19 (1169.8 m).

The results of AMICS show the contact relationship and occurrence state between various minerals. Quartz and feldspar are mainly in the presence of point–line contact. The particles with strong compaction show the way of concave–convex contact. The pores sometimes can be filled with cements, for example, calcite, chlorite and illite. Mica presents bending deformation under strong compaction (Figure 2F,G).

The types and content of rock composition in the Wuqi, Zhidan and Ansai areas are different. Generally, feldspar content is the highest, followed by the content of quartz, and the content of rock fragments is the lowest in the study area. In the Wuqi area, the feldspar proportion is 40.02%, the quartz proportion is 33.53%, and the rock fragments proportion is 19.26%. In the Zhidan area, the feldspar proportion is 44.24%, the quartz proportion is 33.58%, and the rock fragments proportion is 13.75%. In the Ansai area, the feldspar proportion is 50.97%, the quartz proportion is 28.47%, and the rock fragments proportion is 12.80%.

The rock fragments primarily include three types, namely, igneous fragments, metamorphic fragments and sedimentary fragments. Igneous fragments contain granite, eruptive rock and cryptocrystalline rock. Metamorphic fragments contain high metamorphic rock, quartzite, schist, phyllite, slate and metasandstone. Sedimentary fragments contain siltstone, mudstone, dolomite, limestone, chert, and so on. The rock fragments are dominated by metamorphic rock fragments, followed by igneous rock fragments, and sedimentary rock fragments comprises the lowest amount in the study area (Figure 3).

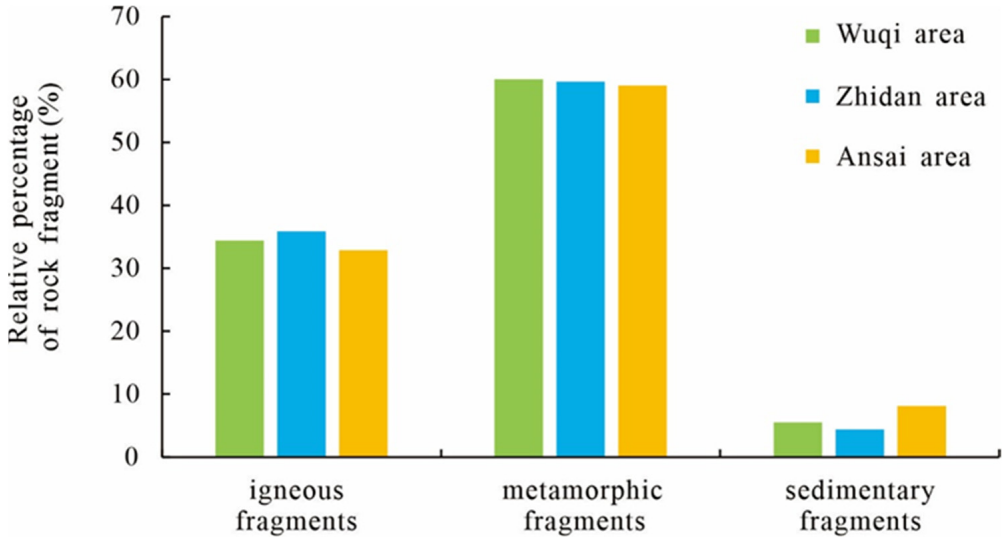


**Figure 3.** Relative percentage of different rock fragment types of Chang 8 Member of the Yanchang Formation tight sandstone reservoirs in study area.

Cement types in the study area mainly include carbonate cements, siliceous cements, clay minerals and mud. The carbonate cements are the dominating cements. Carbonate cements mainly contain calcite, dolomite, ferroan calcite and ankerite. The siliceous cements are quartz secondary overgrowth, or some authigenic quartz grains developed in the pores. Clay mineral cements mainly include chlorite, illite and kaolinite (Figure 4).

### *4.2. Characteristics of Calcite Cements*

#### 4.2.1. Types of Calcite Cements

Carbonate cementation is the primary cementation of the Chang 8 tight sandstone reservoir in the study area. Based on observation and identification of thin sections, it was concluded that there are mainly four types of carbonate cements: calcite, ferroan calcite, dolomite and ankerite. The content of ferroan calcite, ankerite and dolomite is low; they only occur in a few depth intervals of some wells (Figure 5E,F). The carbonate cements in the study area are dominated by calcite cements (Figure 5A–D). Calcite cements usually present porous cementation or basal cementation. In some sandstone intervals, calcite cements are distributed sporadically or dispersedly. The occurrence of calcite cements mainly contains patterns of intergranular filling, metasomatic mineral filling or filled among pores. Calcite cements indirectly contact with quartz, feldspar and other minerals through chlorite coatings, or directly contact with quartz, feldspar and other mineral particles. Some calcite cements are not surrounded by chlorite coatings (Figure 6). Around the pores, it can be seen that some calcite cements are surrounded by chlorite coatings (Figure 5C,D,J), while illite and calcite cements are associated and occur in pores (Figure 5L).

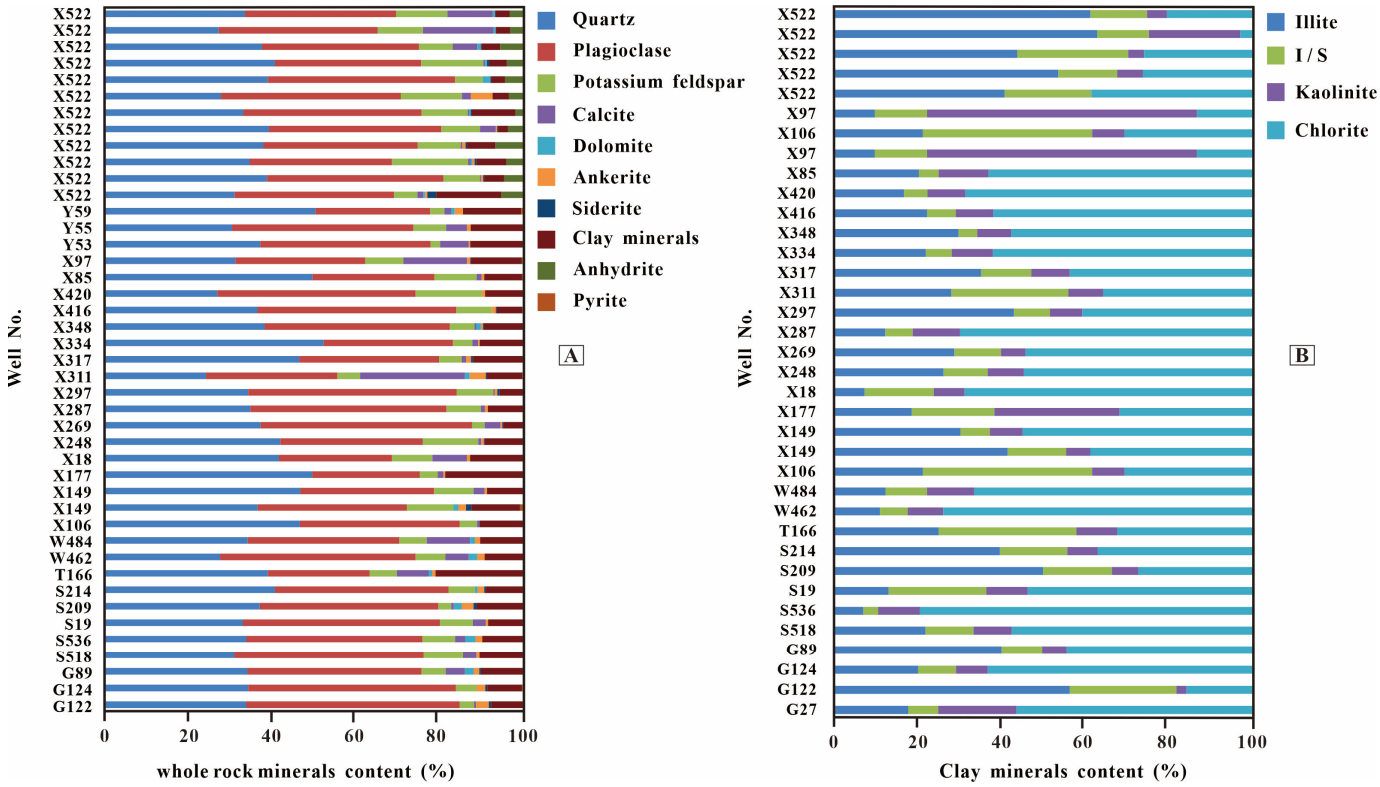


**Figure 4.** Relative percentage of minerals of Chang 8 Member in the Yanchang Formation tight sandstone reservoirs in study area. (**A**) Characteristics of mineral composition of whole rock. (**B**) Characteristics of mineral composition of clay minerals.

According to the observation of cathode luminescence, calcite cements in the study area can mainly be divided into two types based on their characteristics under microscope. The first type with dark-orange luminescence under cathode luminescence generally have no chlorite coatings around them (Figure 5A,B,G). The second type is calcite with bright-yellow luminescence under cathode luminescence, surrounded by chlorite coatings, and showing porous cementation (Figure 5C,D,H,J). Hereinafter, we referred to them as type-I calcite cements and type-II calcite cements.

#### 4.2.2. Distribution of Calcite Cements

The overall carbonate proportion in the study area ranges from 0.20% to 17.25%, with an average of 6.19%. The pattern of cementation distribution is different in the three areas. The occurrence of calcite cements mainly shows porous cementation in the Wuqi and Zhidan areas and shows basal cementation in the Ansai area. Type-I calcite cements present near mudstone or in the interface of sandstone and mudstone. Type-II calcite cements usually occur in the middle and lower part of the fining-upwards sandstone.

The relationship between the two types of calcite cements and the distance to mudstone is shown in Figure 7. Type-I calcite cements' proportion ranges from 4.00% to 17.25%, with an average of 9.83%. Type-II calcite cements' proportion ranges from 0.20–11.28%, with an average of 3.62%. The content of type-I calcite cements is obviously higher than that of type-II calcite cements. Generally, the content of calcite cements decreased gradually with the increase in distance to the mudstone. Additionally, there is obvious negative correlation between the content of calcite cements and its distance to mudstone, which is in accord with the universal phenomenon of carbonate cementation in tight sandstone reservoirs in a lacustrine basin (Figure 7).

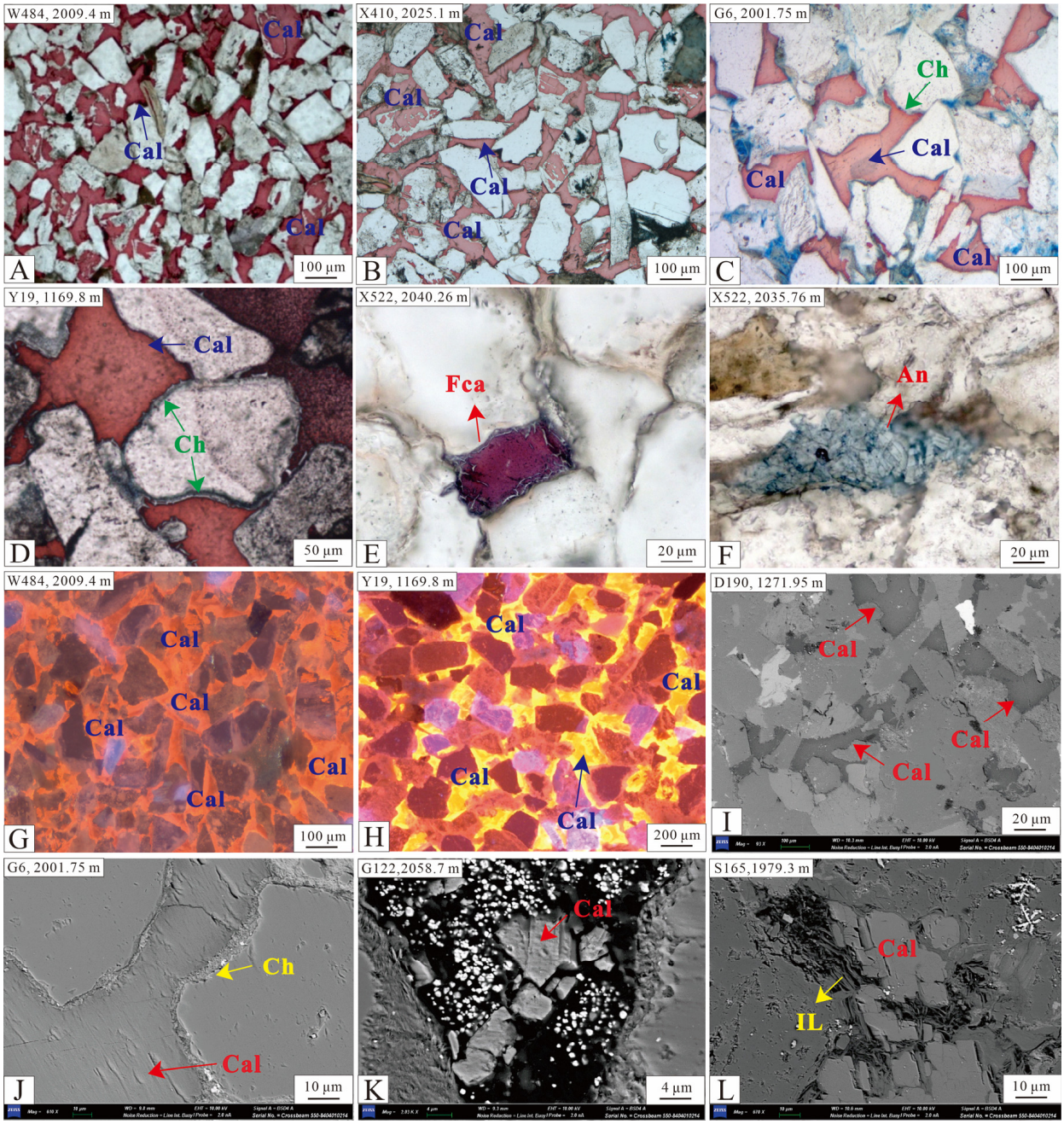


**Figure 5.** Types and characteristics of calcites of Chang 8 Member in the Yanchang Formation in study area. (**A**–**D**) Photomicrographs of thin sections under plane-polarized light suggesting calcites without chlorite coatings in the samples from W484 (2009.4 m) and X410 (2025.1 m) and calcites with the presence of chlorite coatings in the samples from G6 (2001.75 m) and Y19 (1169.8 m), respectively. (**E**,**F**) Photomicrographs of thin sections under plane-polarized light suggesting ferroan calcite and ankerite cements in the samples from X522 (2040.26 m) and X522 (2035.76 m), respectively. (**G**,**H**) CL photomicrographs suggesting type-I calcite cements have dark-orange luminescence color in the samples from W484 (2009.4 m) and type-II calcite cements have bright-yellow luminescence color in the samples from Y19 (1169.8 m), respectively. (**I**,**J**) SEM images suggesting calcites without chlorite coatings in the samples from D190 (1271.95 m) and calcites with the presence of chlorite coatings in the samples from G6 (2001.75 m). (**K**,**L**) SEM images suggesting calcites fill intergranular pores in the samples from G122 (2058.7 m) and S165 (1979.3 m), respectively. (Cal = calcite cements; Ch = chlorite; IL = illite).

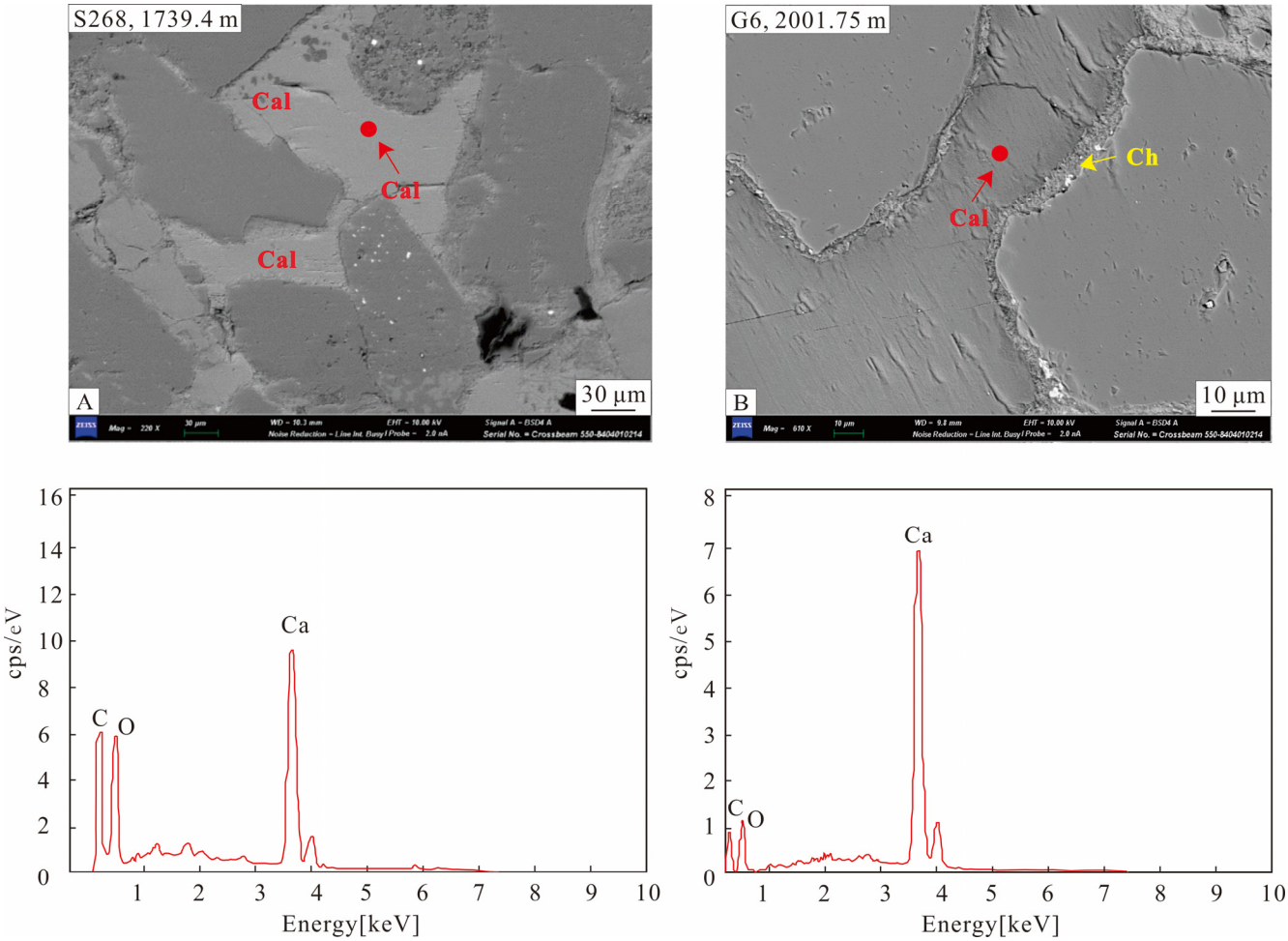


**Figure 6.** BSE images and corresponding energy spectrums characteristic of two types of calcite. (**A**) BSE image of type-I calcites. (**B**) BSE image of type-II calcites. (Cal = calcite cements; Ch = chlorite; red points represent the locations where the EDS analyses were tested).

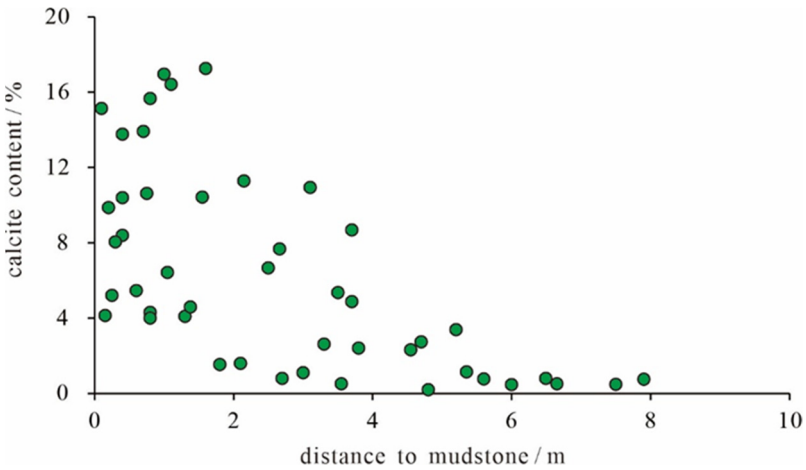


**Figure 7.** Correlation between calcite cement content and the distance to mudstone.

#### 4.2.3. Geochemical Elements Characteristics of Calcite Cements

The element analysis results showed that the major elements in calcite cements are mainly Na, K, Si, Al, etc. The K concentrations in calcite cements range from 0.36 ppm to 3694 ppm, the Al element ranges from 0.15 ppm to 12,298 ppm, the Fe element ranges from

285 ppm to 16,395 ppm, and the Mn element ranges from 2825 to 16,565 ppm. Generally, Fe/Mn values range from 0.07 to 3.51, with an average of 0.98 in the study area. The Fe/Mn values of type-I calcite cements range from 0.07 to 2.06, with an average of 0.22. Type-II calcite cements are surrounded by chlorite coatings, with Fe/Mn values ranging from 0.32 to 3.51; the average value is 1.73. The higher the concentrations of Mn in calcite cements, the brighter yellow of their color under cathode luminescence.

The characteristics of major and trace elements, as well as rare earth elements of the two types of calcite cements are also obviously different. The concentration of Na, K, Si, Al, K, Mg, Fe, Mn, Ti and other elements in type-I calcite cements are obviously higher than that in type-II calcite cements (Figure 8). Type-I calcite cement adjacent to mudstone is rich in LREES, MREES and HREES, and the REES distribution curve is relatively gentle. Type-II calcite cements are also rich in LREES, but relatively poor in MREES and HREES. There are obvious positive and negative Eu anomalies (Figure 9).

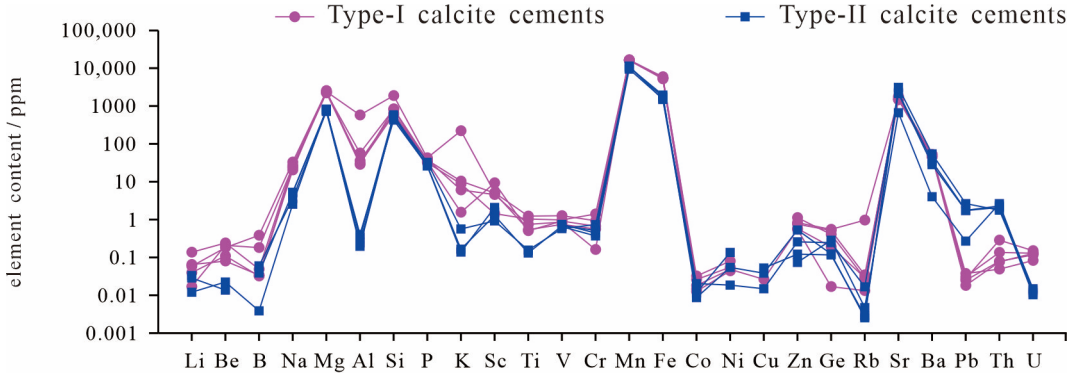


**Figure 8.** Characteristics of major elements and trace elements in two different types of calcite cements. Type-I calcite cements are from samples of W484 (2009.4 m), X522 (2041.06 m), S268 (1796.2 m), D167 (1252.1 m); type-II calcite cements are from samples of G6 (2001.75 m), S165 (1979.85 m), Y19 (1169.8 m).

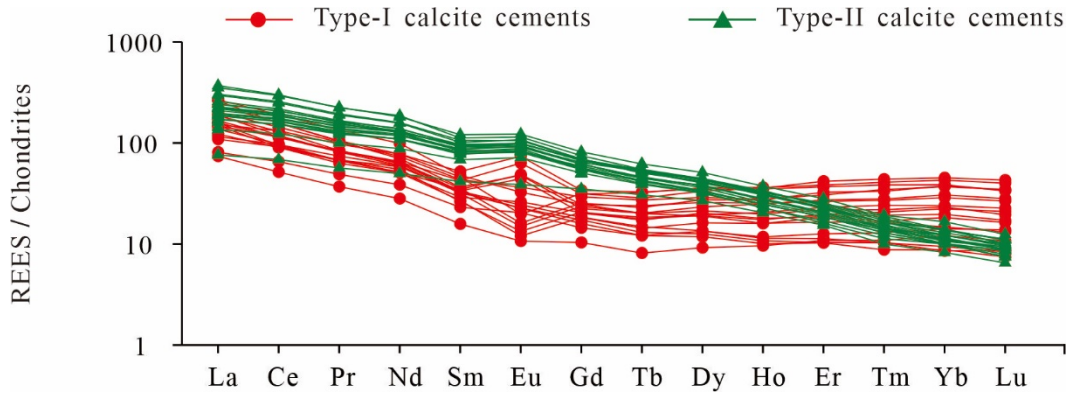


**Figure 9.** Characteristics of rare earth elements of calcite cements. Type-I calcite cements are from samples of W484 (2009.4 m), X522 (2041.06 m), G122 (2065.6 m), X410 (2025.1 m); type-II calcite cements are from samples of G6 (2001.75 m).

#### 4.2.4. Carbon and Oxygen Isotope Characteristics of Calcite Cements

The results of the carbon and oxygen isotopes analysis can be used to indicate the carbon source of calcite cements and its formation temperature. The overall $\delta^{13}C$ values of calcite cements in the study area range from −6.65‰ to 1.84‰, with an average of −1.49‰. The range of $\delta^{18}O$ values are −20.53‰ to −12.28‰, with an average of −18.55‰ in the study area (Figure 10).

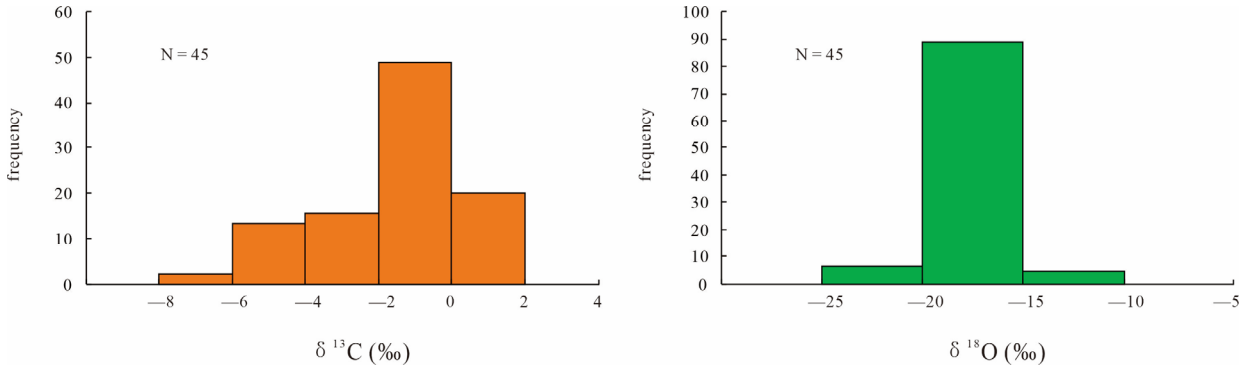


**Figure 10.** Distribution frequency histogram of carbon and oxygen isotopes results of calcite cements.

In type-I calcite cements, the $\delta^{13}C$ values range from −3.13‰ to 0.64‰, with an average value of −0.67‰. The $\delta^{18}O$ values range from −20‰ to −12.28‰, with an average value of −18.83‰. The $\delta^{13}C$ values of type-II calcite cements range from −6.65‰ to 1.84‰, with an average of −2.09‰. The $\delta^{18}O$ values of type-II calcite cements range from −20.53‰ to −13.98‰, with an average value of −19.39‰ (Table 1). The type-II calcite cements have relatively lower $\delta^{13}C$ values. The $\delta^{13}C$ values of type-I calcite cements close to mudstone range from −4‰ to 1‰, which are relatively higher than type-II calcite cements as a whole. The variation range of $\delta^{18}O$ values of the two types of calcite cements are similar, ranging from −20‰ to 12‰ in the study area.

**Table 1.** Results of the carbon and oxygen isotopes of calcite cements.

| Area | Well | Depth/m | Formation | $\delta^{13}C$ (PDB, ‰) | $\delta^{18}O$ (PDB, ‰) | Th/°C |
|---|---|---|---|---|---|---|
| WQ | X522 | 2045.8 | Ch-$8_1$ | −0.57 | −18.05 | 85.52 |
| WQ | X522 | 2041.06 | Ch-$8_1$ | 0.48 | −19.02 | 93.85 |
| WQ | X522 | 2046.4 | Ch-$8_1$ | −2.89 | −18.7 | 91.04 |
| WQ | W484 | 2006.1 | Ch-$8_2$ | −1.42 | −13.98 | 55.87 |
| WQ | W484 | 2006.5 | Ch-$8_2$ | −0.73 | −17.79 | 83.38 |
| WQ | W484 | 2006.7 | Ch-$8_2$ | 0.8 | −19.14 | 94.92 |
| WQ | W484 | 2009.4 | Ch-$8_2$ | −1.47 | −19.07 | 94.30 |
| WQ | G6 | 2001.75 | Ch-$8_2$ | 1.84 | −20.53 | 108.06 |
| WQ | G6 | 1974.85 | Ch-$8_1$ | −3.36 | −19.74 | 100.42 |
| WQ | X318 | 2125.48 | Ch-$8_2$ | −6.65 | −20.25 | 105.30 |
| WQ | X318 | 2128.08 | Ch-$8_2$ | −1.8 | −19.17 | 95.19 |
| WQ | X318 | 1995.15 | Ch-$8_1$ | −0.89 | −19.05 | 94.12 |
| WQ | X410 | 2025.1 | Ch-$8_2$ | −0.19 | −19.82 | 101.18 |
| WQ | X410 | 1993.9 | Ch-$8_1$ | −0.92 | −18.79 | 91.82 |
| WQ | G122 | 2065.8 | Ch-$8_1$ | −1.01 | −18.46 | 88.97 |
| WQ | G122 | 2065.6 | Ch-$8_1$ | −3.13 | −20 | 102.89 |
| ZD | Q147 | 1726.35 | Ch-$8_2$ | −1.48 | −17.99 | 85.02 |
| ZD | Q147 | 1736.02 | Ch-$8_2$ | −1.03 | −18.41 | 88.54 |
| ZD | Q147 | 1735.3 | Ch-$8_2$ | 0.36 | −18.94 | 93.14 |
| ZD | Q147 | 1727.7 | Ch-$8_2$ | 0.64 | −18.52 | 89.48 |
| ZD | Q147 | 1736.6 | Ch-$8_2$ | −0.87 | −17.6 | 81.84 |
| ZD | S98 | 1774.01 | Ch-$8_1$ | −0.36 | −19.81 | 101.08 |
| ZD | S98 | 1774.35 | Ch-$8_1$ | 0.54 | −17.49 | 80.96 |
| ZD | S114 | 1794.5 | Ch-$8_2$ | −0.38 | −15.58 | 66.63 |
| ZD | S114 | 1796.77 | Ch-$8_2$ | −1.48 | −15.41 | 65.43 |
| ZD | S165 | 1971.4 | Ch-$8_2$ | −5.01 | −19.08 | 94.38 |
| ZD | S165 | 1979.85 | Ch-$8_2$ | −5.16 | −19.3 | 96.36 |
| ZD | S165 | 1979.3 | Ch-$8_2$ | 0.27 | −18 | 85.10 |
| ZD | S268 | 1738.35 | Ch-$8_1$ | −0.53 | −17.74 | 82.97 |
| ZD | S268 | 1739.8 | Ch-$8_1$ | 1.18 | −19.21 | 95.55 |
| ZD | S268 | 1748.2 | Ch-$8_1$ | 0.77 | −19.71 | 100.14 |

**Table 1.** *Cont.*

| Area | Well | Depth/m | Formation | $\delta^{13}C$ (PDB, ‰) | $\delta^{18}O$ (PDB, ‰) | Th/°C |
|---|---|---|---|---|---|---|
| ZD | S268 | 1796.2 | Ch-$8_2$ | −0.26 | −18.42 | 88.63 |
| ZD | S268 | 1745 | Ch-$8_1$ | −0.78 | −19.18 | 95.28 |
| AS | D130 | 1671.65 | Ch-$8_2$ | −0.46 | −17.78 | 83.30 |
| AS | D130 | 1668.05 | Ch-$8_2$ | −0.48 | −19.04 | 94.03 |
| AS | D130 | 1672.32 | Ch-$8_2$ | −0.35 | −12.28 | 45.49 |
| AS | D167 | 1252.7 | Ch-$8_2$ | −1.59 | −19.59 | 99.02 |
| AS | D167 | 1252.1 | Ch-$8_2$ | −0.42 | −19 | 93.67 |
| AS | D190 | 1267.2 | Ch-$8_1$ | −3.35 | −18.46 | 88.97 |
| AS | D190 | 1276.05 | Ch-$8_1$ | −2.05 | −19.8 | 100.99 |
| AS | Q124 | 1504.7 | Ch-$8_2$ | −5.12 | −19.52 | 98.38 |
| AS | Q124 | 1504.25 | Ch-$8_2$ | −5.01 | −19.05 | 94.12 |
| AS | Q124 | 1506.78 | Ch-$8_2$ | −2.54 | −19.59 | 99.02 |
| AS | Y19 | 1169.8 | Ch-$8_1$ | −2.45 | −19.99 | 102.79 |
| AS | Y19 | 1176.9 | Ch-$8_1$ | −4.59 | −18.26 | 87.27 |
| AS | Y19 | 1177.35 | Ch-$8_1$ | −4.62 | −19.21 | 95.55 |

The formula $Z = 2.048 \times (\delta^{13}C + 50) + 0.498 \times (\delta^{18}O + 50)$ was used to calculate the carbon and oxygen isotopes data of the calcite cements, and the Z values distribution range from 103.6 to 120.84, with an average of 114.98 in the study area. The Z value can indicate the property of the fluids media when the calcite cement developed in sandstone. If the Z value is over 120, it indicates that it is a marine carbonate type; if the Z value is less than 120, it indicates that it is a freshwater carbonate type; and if the Z value is near the critical value of 120, it indicates that it is a fluid environment where freshwater is continuously mixed. Based on the calculation, the Z values of the calcite cements in the study area are less than 120, suggesting that the fluid property during the formation of the calcite cements was freshwater fluid with high salinity [25].

## 5. Discussion

### *5.1. Formation Time of Calcite Cements*

Fluid inclusions in calcite cements were observed under plane-polarized electron microscopy. The inclusions vary in shapes and sizes. Most of the fluid inclusions have two phases at room temperature: gas phase and liquid phase. The inclusions vary in size, with the range of about 2 μm–10 μm (Figure 11B,F). Some calcite cements have oil and gas attached to their surface, showing light yellow under fluorescence (Figure 11F). Other calcite cements have no oil and gas impregnation and appear dark blue under fluorescence (Figure 11C).

Due to the number of inclusions in calcite cements that can be found under the electron microscope being limited and the temperature measurement results also having deviations, another method was adopted. We used the formula $1000 \times \ln\alpha_{\textbf{Calcite-water}} = 2.78 \times 10^6/T^2 - 2.89$, substituting the oxygen isotope values into the formula to calculate the formation temperature of calcite cements [25]. The specific results can be seen in Table 1.

According to the calculated formation temperature data of the calcite cements above (Table 1), the overall temperature values of calcite cements in the study area range from 45 to 110 °C (Figure 12). The formation temperature values of type-I calcite cements and type-II calcite cements mainly concentrate at 45.49–89.48 °C and 91.03–108.06 °C, respectively. The temperature of calcite cements measured about 105.8 °C at room temperature, which is consistent with the formation temperature calculated by using the oxygen isotope values, proving that the method of calculating the calcite formation temperature by using the formula is reasonable.

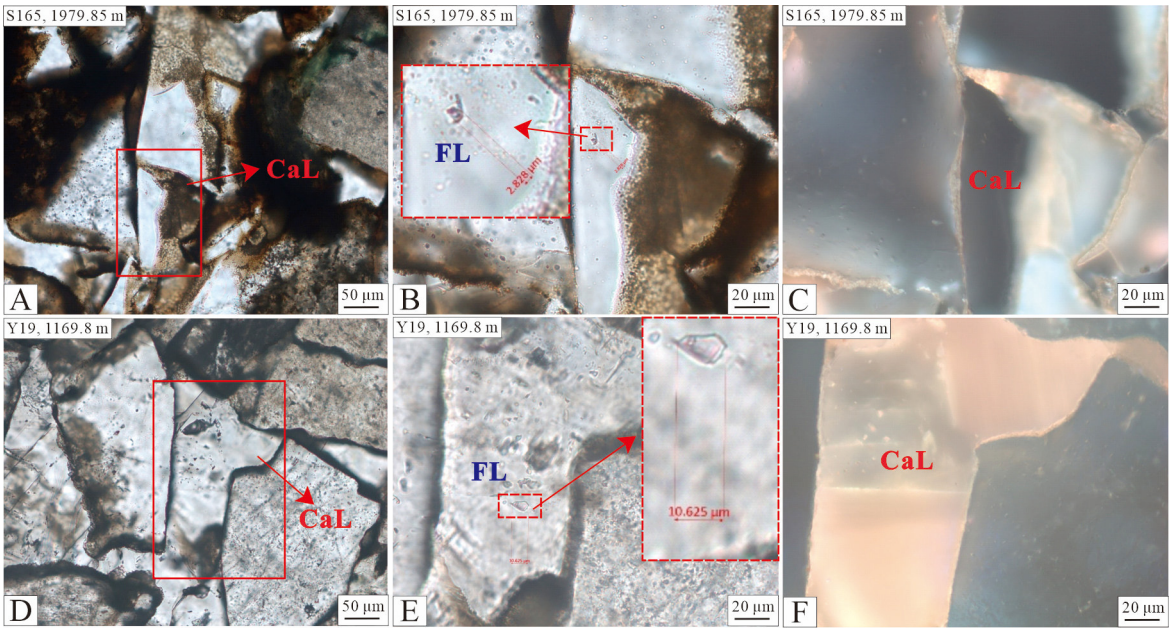


**Figure 11.** Photomicrographs of typical fluid inclusions in calcite cements at room temperature. (**A**–**C**) Sample from S165 (1979.85 m). (**A**) suggesting type-II calcite cements under plane-polarized light and (**B**) is an image under cross-polarized light and (**C**) is an image under fluorescent light. (**D**–**F**) Sample from Y19 (1169.8 m). (**D**) suggesting type-II calcite cements under plane-polarized light and (**E**) is an image under cross-polarized light and (**F**) is an image under fluorescent light.

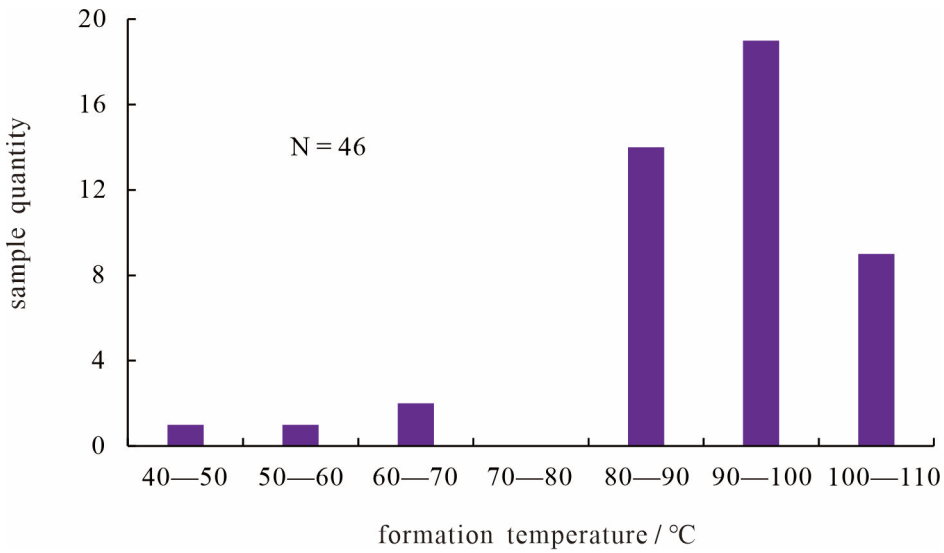


**Figure 12.** Formation temperature of calcite cements in study area recovered by oxygen isotopes results.

Based on the comparison of the two types of calcite cements, the formation temperature of type-I calcite cements, which developed in the early diagenetic period, generally showing basal cementation and filling pore space, is slightly lower,. The formation temperature of type-II calcite cements, which formed during a period of rising temperature, clay minerals were transformed, organic acids were released, and various reactions occurred at a high speed, is relatively higher,. Therefore, type-II calcite cements are generally surrounded by chlorite coatings.

To sum up, the formation time of type-I calcite cements is earlier than that of type-II calcite cements. Organic acids began to decarboxylate and the late period carbon dioxide

formed and entered the sandstone reservoir after the formation temperature rose to over 100 °C. Because the composition and structure of the rocks present at the bottom of the sandstone reservoir is relatively good, for instance, the rocks are rich in quartz and feldspar and poor in mica and cements, some primary pores and other pores can be preserved after strong compaction in this way. After the late period organic acids and other fluids came into the sandstone reservoir, it was easier to preferentially migrate fluids along the places where better pores developed. Carbonate cements precipitated and formed during fluids migration. This accounts for why type-II calcite cements usually occur in the middle and lower part of the sandstone reservoir. The original sandstone with good pore structure was reformed in this process, which led to the densification of the reservoir to a certain extent.

### *5.2. Origin and Genesis of Two Different Types of Calcite Cements*

The source of carbonate cementation is abundant, mainly including internal and external sources. The internal sources refer to the fluids filling in the pores inside the sandstone. The external sources refer to the fluids outside the sandstone and various substances carried by it. Internal sources include the dissolution of carbonate rock fragments and bioclasts, dissolution of anorthite, hydration of primary sedimentary water and aluminosilicate minerals, dissolution of early carbonate cements, metasomatism and the transformation of dark minerals. External sources include diagenesis of organic matter in mudstone, diagenesis of clay minerals and carbonate minerals, dissolution of carbonate minerals outside the sandstone, and external fluids such as deep fluid, atmospheric water and seawater, which can provide sources for carbonate cementation [26–30].

The positive $\delta^{13}C$ values of calcite cements may indicate that their carbon source derives from dissolved carbon in seawater, the dissolution of ocean sedimentary carbonate and lacustrine sedimentary carbonate, atmospheric precipitation, magma and microbial fermentation of organic matter. The negative $\delta^{13}C$ values of calcite cements may indicate that carbon sources include the decarboxylation of organic matter, bacterial oxidation, sulfate reduction of bacteria, hydrothermal methane generation and oxidation, or biogenic methane generation and oxidation [31–34].

On the basis of the petrologic characteristics of the thin sections, there are few carbonate particles and bioclasts in the study area, so it is not regarded as an alternative for the source of carbon for calcite cementation. In combination with the characteristics of the geochemical elements, the origin and genesis of the two types of calcite cements in the study area are discussed.

#### 5.2.1. Type-I Calcite Cements

This type of calcite cementation is mainly distributed in sandstone reservoirs adjacent to the mudstone, or near the interface of sandstone and mudstone. The main feature of type-I calcite cements is that the $\delta^{13}C$ values range from −3.13‰ to 0.64‰, with an average of −0.67‰ (Table 1). The $\delta^{13}C$ value is relatively heavy, indicating that its source belongs to inorganic carbon, it has little relationship with the decarboxylation of organic matter and it may be related to the fluids input from the adjacent mudstone [35–41]. It may also be connected with the precipitation of calcium carbonate in the sedimentary water medium under alkaline conditions [42,43]. The isotopes results suggest that lacustrine carbonates in the adjacent mudstone are the most possible carbon source providers for type-I calcite cementation. In the early diagenesis stage, mudstone was compacted to discharge pore water and other fluids into adjacent sandstone. In addition, the clay minerals in mudstone were also continuously transformed in the early diagenetic period, which released a large amount of ions such as $Ca^{2+}$ and $Mg^{2+}$ into the adjacent sandstone reservoir. With the change of temperature and pressure conditions, the ions precipitated and formed the early carbonate cementation. At this time, the clay minerals in the sandstone reservoir had not been completely transformed and so there was no chlorite coating surrounding the type-I calcite cements.

Cations such as $Al^{3+}$ and $Si^{4+}$ in mudstone are difficult to migrate to sandstone reservoirs with fluids, while $Na^{+}$, $K^{+}$, $Mg^{2+}$ and $Fe^{2+}$ are easy to migrate to adjacent sandstone with fluids. The concentration of Fe in the sandstone reservoir is much higher than that of Mn in the reservoir, which results in higher Fe/Mn values in type-I calcite cements and lower Fe/Mn values in type-II calcite cements. Due to the difficulty of ions migration, the concentration of Fe has obvious positive correlation with the concentration of Mg (Figure 13A), which migrates easily. Additionally, Fe concentration has a weak correlation with the concentration of Al, which does not migrate easily (Figure 13B).

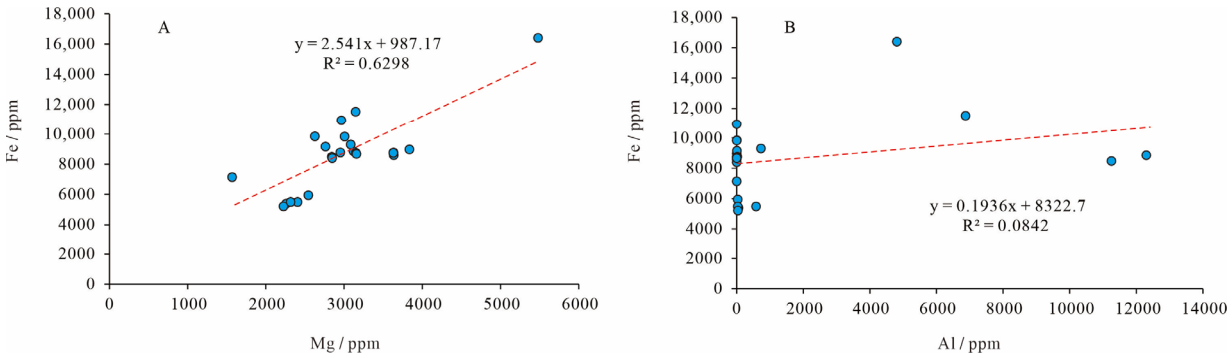


**Figure 13.** Correlation between the concentrations of Fe and Mg and Al in calcite cements. (**A**) Correlation between the concentrations of Fe and Mg. (**B**) Correlation between the concentrations of Fe and Al.

The XRF scanning analysis of the mudstone samples in the study area shows that there are certain carbonate particles in mudstone itself. It can be seen from photomicrographs of the thin sections under plane-polarized light that some micrite carbonates are dyed purplish red by the dye solution (Figure 14A,B). In the process of rapid compaction and burial of the sandstone reservoir, the organic matter gradually matured with the increase of temperature. When the temperature reached about 80–90 °C, the organic acid was released into the pore water of the mudstone, and then the carbonates in the mudstone were dissolved by organic acid to release $Ca^{2+}$, $CO_3^{2-}$, $HCO_3^{-}$, etc. These ions were discharged into the adjacent sandstone reservoir with the continuous compaction and drainage process in the mudstone, and the carbonate cementation was formed by the precipitation of ions. It can be seen from XRF scanning images under SEM that Ca, Fe, Mn elements are obviously present in the same field of vision with the PPL images (Figure 14C–H). This process provides a sufficient material source for calcite cementation in sandstone reservoirs.

### 5.2.2. Type-II Calcite Cements

This type of calcite cementation is mainly distributed in the interior of fine-grained sandstone. The main characteristics are that the $\delta^{13}C$ values range from −6.65‰ to 1.84‰, with an average value of −2.09‰ (Table 1). The $\delta^{13}C$ is relatively light, obviously lower than that of type-I calcite cements, whose average value is −0.67‰. This shows that there may be an organic carbon source involved, which may be related to the decarboxylation of organic matter. The isotope results of samples from the whole study area show that the $\delta^{13}C$ values of type-II calcite cements are obviously lower than those in type-I calcite cements (Figure 15). This suggests that the thermal decarboxylation of organic matter from source rocks is the most likely carbon source for type-II calcite cements. The domain formation temperature interval of type-II calcite cements is 90–100 °C (Figure 12). At this time, the organic matter reaches the mature stage. Carboxylic acid and $CO_2$ released from the pyrolysis of kerogen can provide a carbon source for calcite cements of high quality. Organic acids cause the dissolution of feldspar, mica and other minerals. Ions of $Ca^{2+}$, $Fe^{3+}$, and $Mg^{2+}$ that are released during the transformation of clay minerals can also provide an important material source for the formation of calcite cements.

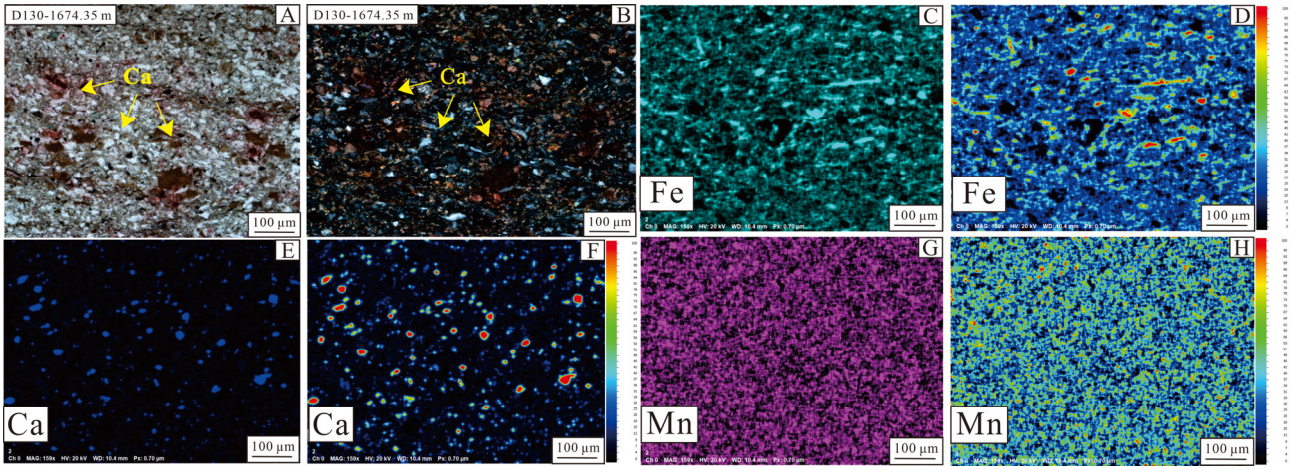


**Figure 14.** X-ray fluorescence distribution characteristics of typical types of elements in calcite cement. (**A**,**B**) Photomicrographs of thin sections under plane-polarized light (**A**) and cross-polarized light (**B**) suggesting the presence of calcite cements in mudstone sample from D130 (1674.35 m). (**C**–**H**) The distribution of typical elements of Fe, Ca, and Mn, respectively.

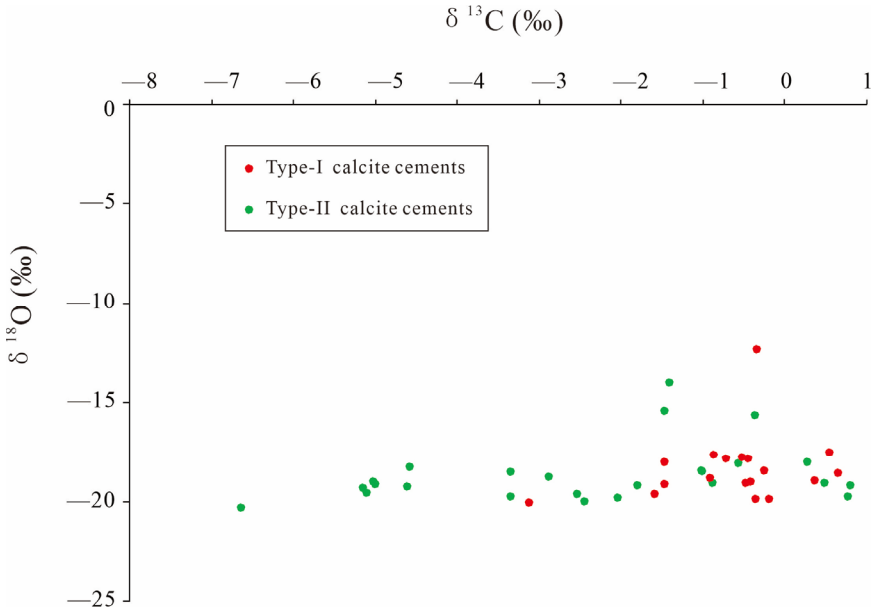


**Figure 15.** The $\delta^{13}C$ and $\delta^{13}O$ values of different types of calcite cements in study area.

The organic matter is deficient in $\delta^{13}C$; the participation of organic matter will reduce the $\delta^{13}C$ value of carbonate cements in the rock. The lower carbon isotope values of some samples in this study may be related to the high amount of doped organic matter in them.

Previous studies have suggested that the binding ability of MREES with carboxylic acids is stronger than that of LREES and HREES [44,45]. Carboxylic acids in source rocks can carry REES into sandstone reservoirs. Thus, the value of ΣLREE/ΣHREE can be used to illustrate the relationship between REES and calcite cements. The values of ΣLREE/ΣHREE in type-II calcite cements are obviously lower than those in type-I calcite cements (Figure 16). This result indicates that the concentration of MREES in type-II calcite cements is relatively high and this may be related to carboxylic acids contained in the fluids carried by the source rock.

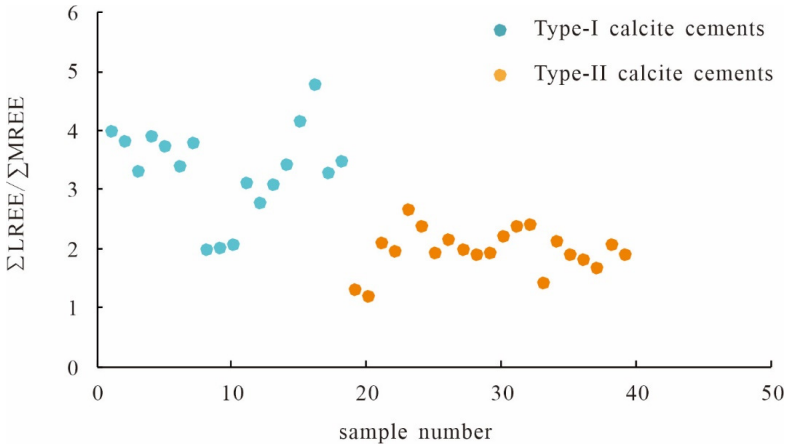


**Figure 16.** Characteristics of rare earth elements of calcite cements in study area.

## 6. Conclusions

The carbonate cements in the tight sandstone reservoirs of the Chang 8 Member of the Yanchang Formation of the Upper Triassic in the Zhijing-Ansai area, Ordos Basin, are mainly calcite cements, and calcite cements can be divided into two types. Type-I calcite cements present near the mudstone or in the interface of sandstone and mudstone. Generally, they arae not surrounded by chlorite coatings. The surrounding pore space is not filled with illite and other clay minerals, showing basal cementation and a dark-orange coloring under cathode luminescence. Type-II calcite cements usually occur in thick sandstone, which is generally surrounded by chlorite coatings. Type-II calcite cements usually occur in the middle and lower part of the fine-grained sandstone, showing porous cementation and a bright-yellow coloring under cathode luminescence.

The contents of Na, K, Si, Al, K, Mg, Fe, Mn, Ti and other elements in type-I calcite cements are obviously higher than those in type-II calcite cements. The REES distribution curve of type-I calcite cements is steep but is relatively gentle in type-II calcite cements. The relative content of MREES and HREES in type-I calcite cements is higher than that in type-II calcite cements.

Lithofacies association and diagenetic fluids evolution jointly control the distribution and difference of calcite cementation. Type-I calcite cements showing basal cementation formed in the early stage. Their formation was mainly influenced by the compaction and diagenetic transformation of adjacent mudstone. Their carbon source may be related to the compaction and drainage of mudstone. Pore fluids discharged from mudstone were precipitated together with calcium in the sandstone reservoir. The carbon source of type-II calcite cements was mainly affected by decarboxylation of organic matter in source rocks.

**Author Contributions:** Conceptualization, K.X. and Z.Z.; data curation—Z.Z., H.Z. and Y.W.; resources—H.X. and C.Y.; funding acquisition—W.D. and B.L.; writing—original draft preparation, Z.Z.; writing—review and editing, Z.Z. All authors have read and agreed to the published version of the manuscript.

**Funding:** This research was funded by the National Natural Science Foundation of China, grant number 42072161, and the Fundamental Research Funds for the Central Universities, grant number 22CX07008A.

**Data Availability Statement:** The data utilized in the study are confidential.

**Acknowledgments:** This paper is supported by Changqing Oilfield Company. We also have a great gratitude to the Research Institute of Petroleum Exploration and Development, Changqing Oilfield Company, PetroChina, for providing core samples, data and permission to publish.

**Conflicts of Interest:** The authors declare no conflict of interest.

## References


1. Wang, X.L.; Zhang, X.L.; Wang, X.; Yang, Z.; Li, Y.J. Characteristics and diagenesis of the Chang 8 tight reservoir of the Yanchang Formation in the central-southern Ordos Basin. *J. North. Univ.* **2021**, *51*, 877–890.
2. Yang, B. *Sedimentary Facies of Chang 9 Oil Formation of the Yanchang Formation in Zhijing-Ansai Area, Ordos Basin*; Northwest University: Kirkland, WA, USA, 2014; Volume 57, pp. 2966–2977.
3. Yu, J.; Zhang, Y.; Zhao, H.T.; Hou, Y.D.; Luo, S.S. Characteristics and evaluation of C-10 reservoir in Zhijing-Ansai area, Ordos Basin. *Geol. Resour.* **2019**, *28*, 364–371.
4. Wang, X.Y.; Liu, N.; Nan, J.X.; Wang, X.L.; Ren, D.Z. Characteristics and Genetic Mechanism of Chang Eight Low Permeability and Tight Reservoir of Triassic Yanchang Formation in Central-East Ordos Basin. *Front. Phys.* **2022**, *743*. [CrossRef]
5. Liu, H.L.; Yang, Y.Y.; Wang, F.Q.; Deng, X.Q.; Liu, Y.; Nan, J.X.; Wang, J.; Zhang, H.J. Micro pore and throat characteristics and origin of tight sandstone reservoirs: A case study of the Triassic Chang 6 and Chang 8 members in Longdong area, Ordos Basin, NW China. *Pet. Explor. Dev.* **2018**, *45*, 239–250. [CrossRef]
6. Liu, G.Z.; Shi, X.Z.; Zhao, Y.G. Characteristics, origin and distribution of carbonate cements in deep-water sand- stones in Huangling area, Ordos Basin. *J. Xi'an Univ. Sci. Technol.* **2021**, *40*, 75–86.
7. Li, Y.; Zhang, W.X.; Li, S.T.; Luo, A.X.; Mou, W.W.; Deng, X.Q.; Yan, C.C.; Hui, X. Characteristics of carbonate cements and their effects on properties in Chang 8 sandstone reservoir, Ordos Basin. *Geol. Sci. Technol. Inf.* **2018**, *37*, 175–183.
8. Yao, J.L.; Wang, Q.; Zhang, R.; Tang, J.; Tian, B.; Liao, P. Origin and spatial distribution of carbonate cements in sandstone of Yanchang Formation in the central Ordos Basin. *Nat. Gas Geosci.* **2011**, *22*, 943–950.
9. Shen, J. Carbonate cementation characteristics and genetic mechanism of tight sandstone reservoirs in Longdong area, Ordos Basin. *Lithol. Reserv.* **2020**, *32*, 24–32.
10. Wang, Z.; Qiu, J.L. Study on composition, carbon and oxygen isotope characteristics of carbonate cements in Chang-8 reservoir, Ordos Basin. *Oil Gas Reserv. Eval. Dev.* **2018**, *8*, 14–21.
11. Leila, M.; Moscariello, A.; Šegvić, B. Depositional facies controls on the diagenesis and reservoir quality of the Messinian Qawasim and Abu Madi formations, onshore Nile Delta, Egypt. *Geol. J.* **2019**, *54*, 1797–1813. [CrossRef]
12. Yousef, I.; Morozov, V.; Sudakov, V.; Idrisov, I. Cementation characteristics and their effect on quality of the Upper Triassic, the Lower Cretaceous, and the Upper Cretaceous sandstone reservoirs, Euphrates Graben, Syria. *J. Earth Sci.* **2021**, *32*, 1545–1562. [CrossRef]
13. Leila, M.; Mohamed, A. Diagenesis and petrophysical characteristics of the shallow Pliocene sandstone reservoirs in the Shinfas Gas Field, onshore Nile Delta, Egypt. *Pet. Explor. Prod. Technol.* **2020**, *10*, 1743–1761. [CrossRef]
14. Morad, S.; Al-Ramadan, K.; Ketzer, J.M.; De Ros, L.F. The impact of diagenesis on the heterogeneity of sandstone reservoirs: A review of the role of depositional facies and sequence stratigraphy. *AAPG Bull.* **2010**, *94*, 1267–1309. [CrossRef]
15. Kassab, M.A.; Hassanain, I.M.; Salem, A.M. Petrography, diagenesis and reservoir characteristics of the Pre-Cenomanian sandstone, Sheikh Attia area, East Central Sinai, Egypt. *J. Afr. Earth Sci.* **2014**, *96*, 122–138. [CrossRef]
16. Xi, K.L.; Cao, Y.C.; Liu, K.Y.; Wu, S.T.; Yuan, G.H.; Zhu, R.K.; Zhao, Y.W.; Hellevang, H. Geochemical constraints on the origins of calcite cements and their impacts on reservoir heterogeneities: A case study on tight oil sandstones of the Upper Triassic Yanchang Formation, southwestern Ordos Basin, China. *AAPG Bull.* **2019**, *103*, 2447–2485. [CrossRef]
17. Zhong, J.Y.; He, M.; Zhou, T.; Huang, H. Origin analysis of carbonate cements in Yangchang Fm. (Triassic) sandstones within the lacustrine center of Ordos Basin, NW China. *Lithol. Oil Gas Reserv.* **2011**, *23*, 65–69.
18. Hu, J.; Wang, G.M.; Wang, C.; Zheng, X.Y. Content variation of calcite and laumontite cement and its control on the difference of lower part of Yanchang Formation tight reservoir in Zhidan-Ansai, China. *J. Chengdu Univ. Technol.* **2020**, *47*, 129–140.
19. Zhang, Y.Y.; Huang, S.J. Characteristics of calcite cements of Chang-6 oil reservoir set in Huaqing area. *Lithol. Reserv.* **2012**, *24*, 48–52+71.
20. Zhang, Y.; Dai, R.; Luo, S.S.; Lyu, Q.Q.; Liu, Y.Q.; Zhao, Q.; Liu, Y. Characteristics and its main controlling factors of Chang 10 reservoir in Yanchang Formation in Zhijing-Ansai area, Ordos Basin. *Chin. Sci. Technol. Pap.* **2018**, *13*, 1029–1035.
21. Shan, Y.P.; Wang, H.J.; Zhang, L.J.; Bai, Z.H.; Su, P.H.; He, Y.X.; Meng, W.K.; Liu, H.Y.; Cheng, M.W. The principle and fast drawing of ternary plots and their application in sandstone classification. *J. Sedimentol.* **2022**, *40*, 1095–1108.
22. Chen, Y.T.; Liu, L.F.; Wang, M.Y.; Dou, W.C.; Xu, Z.J. Characteristics and controlling factors of Chang 6 and Chang 7 reservoirs in southwestern Ordos Basin. *Lithol. Oil Gas Reserv.* **2020**, *32*, 51–65.
23. Fu, J.H.; Deng, X.Q.; Wang, Q.; Li, J.H.; Qiu, J.L.; Hao, L.W.; Zhao, Y.D. Compaction and hydrocarbon accumulation of Triassic Yanchang Formation Chang 8 Member, Ordos Basin, NW China: Evidence from geochemistry and fluid inclusions. *Pet. Explor. Dev.* **2017**, *44*, 48–57. [CrossRef]
24. Hu, R.N. *Diagenetic Differences and its Genesis of Low Permeability Sandstone Reservoirs in the Yanchang Formation, Ordos Basin*; China University of Petroleum: Shandong, China, 2018.
25. Friedman, N.; O'Neil, J.R. *Compilation of Stable Isotope Fractionation Factor*; Professional Paper; US Geological Survey: Baltimore, MD, USA, 1977; pp. 440–450.
26. Zhang, Q.Q.; Liu, K.Y.; Liu, T.X.; Sun, R.P.; Meng, Y. Research status of the genesis of carbonate cementation in clastic reservoirs. *Mar. Oil Gas Geol.* **2021**, *26*, 231–244.
27. Tang, J.; Johannesson, K.H. Ligand extraction of rare earth elements from aquifer sediments: Implications for rare earth element complexation with organic matter in natural waters. *Geochim. Et Cosmochim. Acta* **2010**, *74*, 6690–6705. [CrossRef]

28. Li, W.M.; Zhang, T.C.; Zhong, Y.M.; Yang, Y.J.; Nan, H.L. Formation mechanism of sandstone cements in sandstone of the Xujiahe Member 4 in western Sichuan Depression: Evidence from trace elements. *Mar. Oil Gas Geol.* **2022**, *27*, 175–184.
29. Tang, C.; Sima, X.Z.; Zhu, Q.; Feng, X.X.; Chen, Y.; Chen, L.L.; Liu, X.X. Carbon and oxygen isotopic composition and uranium mineralization significance of calcite of Zhiluo Formation uranium-bearing sandstones in Dongsheng area. *J. Univ. Geol.* **2016**, *22*, 698–706.
30. Guo, H.L.; Wang, D.R. Tarim expected the isotopic composition of sandstone reservoir in carbonate cements and cause analysis. *Pet. Explor. Dev.* **1999**, *26*, 31–32.
31. Tian, Y.M.; Shi, Z.J.; Song, J.H.; Wu, X.M.; Gao, X.; Hong, C.Y. Characteristics of carbonate cements of Member 8 of Yanchang Formation in the Yichuan-Xunyi area, Ordos Basin, China. *J. Chengdu Univ. Technol.* **2011**, *38*, 378–384.
32. O'Neil, J.R.; Clayton, R.N.; Mayeda, T.K. Oxygen isotope fractionation in divalent metal carbonates. *J. Chem. Phys.* **1969**, *51*, 5547–5558. [CrossRef]
33. Song, T.; Ma, F.; Liu, L.; Meng, Q.A.; Yu, Y.L.; Liu, N.; Yu, M. Features and genesis of carbon and oxygen isotopes in calcite cement from sandstone in oil-bearing Fuyu layer of Daqing Placanticline. *Pet. Nat. Gas Geol.* **2015**, *36*, 255–261.
34. Mao, L.L.; Yi, H.S.; Ji, C.J.; Xia, G.Q. Petrology and carbon and oxygen isotope characteristics of the Cenozoic lacustrine carbonate rocks in Qaidam Basin. *Geol. Sci. Technol. Inf.* **2015**, *33*, 41–48.
35. Jiang, S.Y.; Chen, W.; Zhao, K.D.; Zhang, D.; Lu, Y.; Zhao, H.D. In situ micro-analysis of isotopic compositions of solid minerals using LA-(MC)-ICP-MS methods and their application. *J. Mass Spectrom.* **2021**, *42*, 623–640.
36. Zhou, X.F.; Li, Y.D.; Wang, W.; Sang, T.Y.; Yu, J.M. New ideas on identification method of calcite and dolomite cements: Taking Yanchang Formation sandstones in Ordos Basin as an example. *J. Xi'an Pet. Univ.* **2019**, *34*, 15–20.
37. Wang, Y.T.; Sun, G.Q.; Zhang, S.C.; Chen, B.; Zhu, W.J.; Jiang, Y. Characteristics and genesis of carbonate cement in abdomen sandstone in northern margin of Qaidam Basin. *Nat. Gas Geosci.* **2021**, *32*, 1037–1046.
38. Song, K.P.; Luo, J.L.; Liu, X.S.; Hou, Y.D.; Sheng, W.Y.; Cao, J.J.; Mao, Q.R. Characteristics and genetic mechanism of carbonate cements in Upper Paleozoic tight sandstones, southwestern Ordos Basin. *Nat. Gas Geosci.* **2020**, *31*, 1562–1573.
39. Wei, W.; Zhu, X.M.; Zhu, S.F.; He, M.W.; Sun, S.Y.; Zhao, X.Z.; Wu, J.P.; Wang, M.W. Marine & Petroleum Geology. In *Petrographic and Origin of Authigenic Carbonate Minerals and the Associated Fluid Evolution in the Lacustrine Carbonate-Siliciclastic Mudrocks: A Case from the Low Cretaceous of the Erennaoer Sag, Erlian Basin, NE China*; Elsevier: Amsterdam, The Netherlands, 2016.
40. Yang, X.Y.; Luo, X.D.; Ling, M.X. Study on C-O isotope of carbonate cement of uranium bearing sandstone in Ordos Basin and its geological significance. *J. China Univ. Sci. Technol.* **2007**, *8*, 979–985.
41. Liu, S.B.; Huang, S.J.; Shen, Z.M.; Lyu, Z.X.; Song, R.C. Diagenetic fluid evolution and water-rock interaction model of carbonate cements in sandstone: An example from the reservoir sandstone of the Fourth Member of the Xujiahe Formation of the Xiaoquan-Fenggu area, Sichuan Province, China. *Sci. China: Earth Sci.* **2014**, *57*, 1077–1092. [CrossRef]
42. Cui, J.W.; Zhu, R.K. Mechanism of strong calcium cementation in tight sandstone and its significance: A case study on Triassic Chang 7 oil Formation of Yangchang Formation in Ordos Basin. *J. Jilin Univ.* **2020**, *50*, 957–967.
43. Pang, J.G.; Guo, J.A.; Yang, Y.Y.; Dong, Y.; Shang, X.Q.; Wang, G.C.; Li, Q. The formation mechanism of multi-stage carbonate cements in tight sandstone: A case study of Chang $6_3$ sub-Member of Triassic Yanchang Formation in Huaqing area, Ordos Basin. *Geol. Bull. China* **2018**, *37*, 930–937.
44. Lin, M.R.; Wang, Y.Z.; Cao, Y.C.; Wang, S.P.; Xie, Q.W.; Dong, X.Y. Sources of $Ca^{2+}$ in the major carbonate cements in Eocene sandstones and conglomerates: Evidence from Sr isotopes, Sr/Ca ratios, and rare-earth elements. *Mar. Pet. Geol.* **2020**, *120*, 104568.
45. Wu, S.T.; Xu, C.X.; Chen, Z.D.; Wang, Y.P.; Bai, J.F. Rapid determination of Mg, Ca, Sr, Ba and LREEs in carbonate by laser ablation-inductively coupled plasma-mass spectrometry in combination with high pressure tableting technology. *Anal. Lab.* **2019**, *38*, 1089–1094.